Graefe's Archive for Clinical and Experimental Ophthalmology (2021) 259:1297–1308
https://doi.org/10.1007/s00417-020-05023-w

NEUROPHTHALMOLOGY

Correlations between visual morphological, electrophysiological, and acuity changes in chronic non-arteritic ischemic optic neuropathy

Lucilla Barbano[1] · Lucia Ziccardi[1] · Vincenzo Parisi[1]

Received: 6 May 2020 / Revised: 9 October 2020 / Accepted: 19 November 2020 / Published online: 7 January 2021

Abstract

Purpose To study whether there is a correlation between the macular and optic nerve morphological condition and the retinal ganglion cells (RGCs) and visual pathways' function, and to investigate whether visual acuity (VA) changes might be related to the morpho-functional findings in chronic non-arteritic ischemic optic neuropathy (NAION).

Methods In this retrospective study, 22 patients (mean age 62.12 ± 6.87) with chronic unilateral NAION providing 22 affected and 22 fellow eyes without NAION (NAION-FE), and 20 (mean age 61.20 ± 7.32) healthy control subjects were studied by spectral domain optical coherence tomography (Sd-OCT) for investigating macular thickness (MT) and volume (MV) of the whole (WR), inner (IR) and outer retina (OR), and the peripapillary retinal nerve fiber layer thickness (RNFL-T) measured overall and for all quadrants. Also, simultaneous 60′ and 15′ pattern electroretinogram (PERG) and visual evoked potentials (VEP) and VA were assessed. Differences of MT and MV of WR, IR, OR, and RNFL-T overall and for all quadrants, PERG amplitude (A), VEP implicit time (IT), and A and VA values between NAION eyes and controls were assessed by one-way analysis of variance. Pearson's test was used for regression analysis. A p value < 0.01 was considered as significant.

Results In NAION eyes as compared to NAION-FE eyes and controls, significant ($p < 0.01$) changes of MT, MV of WR and IR, RNFL-T, 60′ and 15′ PERG A, VEP IT and A, and VA were found. No significant ($p > 0.01$) OR changes were observed between groups. In NAION eyes, significant ($p < 0.01$) correlations between MV of WR and IR and 15′ PERG A were found. Overall, RNFL-T values were significantly correlated ($p < 0.01$) with those of 60′ PERG A and VEP IT and A; temporal RNFL-T values were correlated ($p < 0.01$) with 15′ PERG A and VEP IT and A ones. Temporal RNFL-T, MV-IR, and 15′ PERG A as well as VEP IT were significantly ($p < 0.01$) correlated with VA. Significant ($p < 0.01$) linear correlations between 60′ and 15′ PERG A findings and the corresponding values of 60′ and 15′ VEP A were also found.

Conclusion Our findings suggest that in chronic NAION, there is a morpho-functional impairment of the IR, with OR structural sparing. VA changes are related to the impaired morphology and function of IR, to the temporal RNFL-T reduction and to the dysfunction of both large and small axons forming the visual pathway.

Keywords Ischemic optic neuropathy · Sd-OCT · PERG · VEP

✉ Lucia Ziccardi
lucia.ziccardi@fondazionebietti.it

[1] Visual Neurophysiology and Neurophthalmology Unit, IRCCS - Fondazione Bietti, Via Livenza 1, 00198 Rome, Italy

Key messages

- Although it is known that in chronic non-arteritic ischemic optic neuropathy (NAION) a morphological and functional impairment of RGCs and of the neural conduction along the visual pathways coexist, there is lack of integrated information about the impact of this impairment on visual acuity.
- In chronic NAION, we observed a morpho-functional impairment of the inner retina, with outer retina structural sparing.
- In chronic NAION, visual acuity changes were related to the impaired morphology and function of inner retina, to the temporal thickness reduction of retinal nerve fiber layer and to the dysfunction of both large and small axons forming the visual pathway.

Introduction

Non-arteritic anterior ischemic optic neuropathy (NAION) is the most common cause of non-glaucomatous optic neuropathy in adults over 50 years [1]. It is characterized by a painless and acute vascular failure of the optic nerve, with optic nerve head swelling (more often in small discs with no cupping), sudden loss of visual acuity (VA), and remarkable visual field (VF) defects [1, 2].

In the chronic phase, as a consequence of the acute ischemic injury, the optic nerve head swelling ends in a sectorial or diffuse pallor. A morphological and functional impairment of the retinal ganglion cells (RGCs) and their fibers, forming the optic nerve [3, 4], occurs in a period between 1 and 6 months after the onset of the pathology [3]. Our recent evidence suggests that this neurodegenerative process may not be considered irreversible, since it can be in part stabilized or reduced by the administration of citicoline in oral solution [5].

The morphological assessment of the RGCs and of their fibers can be performed in vivo by spectral domain optical coherence tomography (Sd-OCT). In particular, since a greater proportion of RGCs are enclosed into the inner retinal layers (IR) of the macula, the measurement of macular thickness (MT) and macular volume (MV) could represent a reliable method to assess the entire morphological involvement consequent to the ischemic degeneration [6]. Nevertheless, since the RGCs constitute about 34% of the overall MT [7], the evaluation of MT and MV, further segmented in outer retina (OR) and in IR, may represent a more appropriate method for assessing RGCs involved in the degeneration [6, 7]. The morphology of the RGCs' axons, forming the optic nerve, can be evaluated by Sd-OCT measurement of retinal nerve fiber layer thickness (RNFL-T) [8–13]. Several studies reported that, as expected, a hallmark of the chronic phase of NAION is the reduction of RNFL-T [2, 11, 14–16], of MT [15, 17, 18] and of MV [15].

The functional evaluation of RGCs and their fibers, and of the whole visual pathways, can be performed by pattern electroretinogram (PERG) and visual evoked potential (VEP) recordings, respectively [19]. Indeed, by using appropriate visual stimuli, it is possible to discriminate the neural conduction along the larger or the smaller axons composing the visual pathways [19–21]. These electrophysiological methods have allowed to quantify and distinguish the dysfunction driven by RGCs [4, 22–25] or by the optic nerve [4, 22, 23] that occurs in the chronic phase of NAION.

Since in chronic NAION there is a progressive visual dysfunction, an interesting and actual topic may be to evaluate whether the changes in VA are related to a morphological involvement (changes in Sd-OCT RNFL-T, MT, and MV) and/or RGCs and visual pathway dysfunction (changes in PERG and VEP responses). In these patients, a significant relationship between the reduction of RGCs and RNFL-T and the progression of the loss of VA [13, 14, 17, 26, 27] has been reported. By contrast, there is lack of comprehensive evidences about the potential correlation between the dysfunction of RGCs and VA data and the abovementioned morphological changes.

Therefore, we aimed to study whether there is a correlation between the macular and optic nerve fiber morphological involvement (assessed by Sd-OCT MT and MV and RNFL-T measurements) and the RGCs and visual pathways' function (evaluated by PERG and VEP recordings, respectively), and to investigate whether VA changes might be related to this morpho-functional condition in the chronic phase of NAION.

Materials and methods

This research was designed as a monocentric and retrospective study. The study followed the tenets of the Declaration of Helsinki, and was approved by the local ethics committee on February 14, 2017 (Comitato Etico Centrale IRCCS Lazio, Sezione IFO/Fondazione Bietti, Rome, Italy). Upon recruitment, executed from February to July 2017, at the IRCCS-Fondazione Bietti, each patient signed the informed consent.

Twenty-two patients (14 females and 8 males) affected by unilateral NAION (mean age 62.12 ± 6.87 years) providing 22

eyes with NAION (NAION group), 22 fellow eyes without NAION (NAION-FE group), and 20 age-matched (12 females and 8 males) healthy control subjects (control group, mean age 61.20 ± 7.32 years, 20 eyes) participated to the study. Based on the inclusion/exclusion criteria (see below), enrolled patients were selected from a larger cohort of 137 patients with NAION.

All subjects underwent an extensive ophthalmologic evaluation, including best-corrected VA measured as logarithm of the minimum angle of resolution (LogMAR), slit-lamp biomicroscopy, intraocular pressure (IOP) measurement, indirect ophthalmoscopy, optic nerve head 30° color standard photography, Humphrey 30–2 automated visual field test (HFA 30–2), Sd-OCT scans (with analysis of RNFL-T, MT, and MV), PERG, and VEP recordings.

Inclusion criteria for NAION patients were age > 45 years; disease persisting at least 6 months [3] after an acute episode of sudden, painless, unilateral visual loss, VA < 0.8 LogMAR and diffuse/altitudinal scotoma VF defects with a mean deviation > − 5 dB; IOP < 18 mmHg; no abnormalities of the anterior segment; presence of ophthalmoscopic sign of pale optic disc head with absence of optic disc edema or RNFL swelling (evaluated by Sd-OCT, see below). Exclusion criteria were the presence of clinical and laboratory data leading to Horton's disease; history or presence of any other type of optic neuropathy (glaucomatous, demyelinating, inflammatory, toxic, or hereditary); presence of fluorescein angiography sign of any type of retinal vasculopathy (i.e., central vein/artery occlusion); intake of drugs with potential neuroprotective effects (i.e., brimonidine tartrate [28], coenzyme-Q10 [29], citicoline [5]) at least 12 months prior to the enrolment in the present study. Excluded from the present study were also all NAION patients with VF centrocecal scotoma that did not allow perceiving the target of PERG and VEP stimuli (see below). In addition, since the high myopia can influence the PERG responses [30], eyes with a refractive error greater than 3 negative diopters were also excluded.

For NAION, NAION-FE, and control eyes, exclusion criteria were presence of moderate to dense lens and corneal opacities or maculopathy which are known to affect PERG and VEP responses [31], previous history of refractive surgery, glaucoma or ocular hypertension, intraocular inflammation such as anterior or posterior uveitis, retinal detachment or laser treatment for peripheral retinal diseases, ocular trauma, diabetes, and other systemic or neurological diseases.

In all enrolled patients (NAION or NAION-FE eyes) and controls, the following examinations were performed.

Visual acuity assessment

Best-corrected VA was evaluated by the modified self-illuminated Early Treatment Diabetic Retinopathy Study (ETDRS) charts (Lighthouse, Low Vision Products, Long Island City, NY, USA) at the distance of 4 m. VA was measured as LogMAR.

Spectral domain optical coherence tomography analysis

MT, MV, and RNFL-T were assessed using RTVue-100 Sd-OCT device (RTVue Model-RT100 version 6.3; Optovue Inc., Fremont, CA, USA) according to APOSTEL recommendations [32].

Macular thickness and volume The morphology of the macular area can be explored in vivo by Sd-OCT, providing layer-by-layer objective measurements of anatomical structures. Sd-OCT scans were obtained in a dark room after pupil dilation with tropicamide 1% drops and each scan was carefully reviewed for the accurate identification and segmentation of the retinal layers by two expert graders (LZ and LB) to exclude cases of failed segmentation. The Sd-OCT image quality signal strength index of the acquired scan was at least 40. Scans that did not fulfill the above criteria were excluded from the analysis. The RTVue-100 device uses a low coherence light source centered at 840 nm with 50 nm bandwidth, which gives an axial resolution of 5 μm.

By using the MM5 protocol, we collected MT and MV data from the ETDRS map. The MM5 grid scanning protocol consists of 11 horizontal lines with 5 mm scan length, 6 horizontal lines with 3 mm scan length, 11 vertical lines with 5 mm scan length, 6 vertical lines with 3 mm scan length each at 0.5 mm interval, all centered at the fovea. The number of A-scans in long horizontal and vertical line is 668 and the number of A-scans in short horizontal and vertical line is 400. This scan configuration provided an acquisition rate of 26.000 A-scans/second.

The segmentation algorithm of the MM5 scanning protocol also enables the automatic segmentation of the outer retinal thickness and volume (MT-OR and MV-OR), of the inner retinal thickness and volume (MT-IR and MV-IR), and whole retinal thickness and volume (MT-WR and MV-WR) of the macular region.

The software automatically divides the inner and outer neurosensory retinas at the boundary between the inner nuclear layer (INL) and the outer plexiform layer (OPL). The OR encloses the OPL, the outer nuclear layer and the photoreceptor layer. The IR examines the RNFL, the complex of RGCs and inner plexiform layer (GC/IPL) and the INL. The boundaries of the OR were the anterior of the OPL and the photoreceptor inner segment/outer segment junction. The following boundaries were identified for the IR segmentation: the inner limiting membrane and the posterior of the INL.

Retinal nerve fiber layer thickness Peripapillary RNFL 3.45 protocol was used. The characteristics of Sd-OCT evaluation are reported extensively in our previous work [33]. In the Sd-OCT results, we considered the average value of RNFL thickness of the following quadrants: superior (RNFL-ST), inferior (RNFL-IT), nasal (RNFL-NT), and temporal (RNFL-TT); the overall data obtained in all quadrants (average of 8 values) were identified as RNFL overall (RNFL-OT).

Electrophysiological (PERG and VEP) assessment

Simultaneous PERG and VEP recordings were performed using a previously published method [5, 19–21]. Briefly, the visual stimulation was monocular after occlusion of the other eye and the visual stimuli were checkerboard patterns (contrast, 80%; mean luminance, 110 cd/m^2) generated on a TV monitor and reversed in contrast at the rate of two reversals per second. At the viewing distance of 114 cm, the check edges subtended 60 min (60′) and 15 min (15′) of the visual angle. We used two different checkerboard patterns, as suggested by the VEP ISCEV standards [34], to obtain a prevalent activation of larger (60′ checks) or smaller (15′ checks) axons [20, 21]. The monitor screen subtended 23°. A small fixation target, subtending a visual angle of approximately 0.5° (estimated after taking into account spectacle-corrected individual refractive errors), was placed at the center of the pattern stimulus. For every PERG and VEP acquisition, each patient positively reported that he/she could clearly perceive the fixation target.

The PERG bioelectrical signal was recorded by a small Ag/AgCl skin electrode placed over the lower eyelid. PERGs were bipolarly derived between the stimulated (active electrode) and the patched (reference electrode) eye. A discussion on PERGs using skin electrodes and its relationship to the responses obtained by corneal electrodes can be found elsewhere [35, 36]. In the PERG response, we considered peaks having the following implicit times: 50 and 95 msec (P50, N95); the peak-to-peak amplitude between P50 and N95 was measured (PERG A). In the VEP response, we considered and measured peaks having the following implicit times (IT): 75 and 100 msec (N75 and P100) and the peak-to-peak amplitude between N75 and P100 (VEP A).

During a recording session, simultaneous PERG and VEP were recorded at least twice (between 2 to 6 times) and the resulting waveforms were superimposed to check the repeatability of results. On the basis of our previous study [37], we know that intra-individual variability (evaluated by test-retest) is approximately ± 2 msec for VEP P100 IT and approximately ± 0.18 microvolts for PERG A. During the recording session, we considered as "superimposable," and therefore repeatable, two successive waveforms, with a difference in msec (for VEP P100 IT) and in microvolts (for PERG A) that was less than the above reported values of intra-individual variability. At times, the first two recordings were sufficient to obtain repeatable waveforms, while other times, further recordings were required (albeit never more than 6 in the cohort of patients). For statistical analyses (see below), we considered PERG and VEP values measured in the recording with the lowest PERG A.

In each patient, the signal-to-noise ratio (SNR) of PERG and VEP responses was assessed by using our previously published methods [20, 21, 37]. We accepted VEP and PERG signals with a SNR > 2 for all subjects.

Statistical analysis

We assumed a Gaussian distribution of our data. The normal distribution was assessed by using the Kolmogorov-Smirnov test. Size estimates were obtained from pilot evaluations performed in 13 eyes from 13 NAION eyes, and 12 eyes from 12 control subjects, other than those included in the current study (unpublished data). Inter-individual variability, expressed as standard deviation (SD) data, was estimated for 15′ PERG A. For PERG A, Mean/SD ratio value was higher for NAION (mean 1.35 microvolt; SD 0.32 microvolt, about 24% of the mean) than for controls (mean 2.65 microvolt; SD 0.30 microvolt, about 11% of the mean). It was also established that, assuming the above mean and SD values, sample sizes of control subjects and NAION patients provided a power of 80% ($\beta = 20\%$) at $\alpha = 5\%$ for detecting a between-group difference of 11% in PERG A measurement. Thus, a sample size of 18 NAION patients and 18 control subjects was obtained.

For VA, PERG, VEP, and Sd-OCT parameters, 95% confidence limits were obtained from control data by calculating mean values + 2 SD for VEP IT and mean values − 2 SD for PERG A, VEP A, MT, MV, and RNFL-T (see Table 1). VA was considered as abnormal for values greater than 0.0 LogMAR.

Differences of VA, PERG, VEP, and Sd-OCT values between controls and NAION or NAION-FE groups were evaluated by the one-way analysis of variance (ANOVA). Pearson's test was applied to compare morphological (RNFL-T, MT, and MV), electro-functional (PERG A, VEP IT, and VEP A), and VA data.

In all analyses, we considered as statistically significant a p value lower than 0.01. Minitab 17 (version 1) software was used for statistics.

Results

Figure 1 shows representative example of PERG and VEP recordings and RNFL-T in one control eye (#7) and one NAION eye (#10).

Table 1 Individual data of visual acuity (VA), macular thickness (MT), macular volume (MV), retinal nerve fiber layer (RNFL) thickness, 60′ and 15′ pattern electroretinogram (PERG) P50-N95 amplitude (A), visual evoked potentials (VEP) P100 implicit time (IT) and N75-P100 amplitude (A), detected in patients with non-arteritic ischemic optic neuropathy (NAION, 22 eyes). *60′ and 15′*, visual stimuli checks subtending 60 and 15 min of visual arc, respectively; *WR*, whole retina; *IR*, inner retina; *OR*, outer retina, *TT*, temporal thickness; *ST*, superior thickness; *IT*, inferior thickness; *NT*, nasal thickness; *OT*, overall thickness; *μ*, microns; *μV*, microvolt; *msec*, milliseconds; *CL*, 95% normal confidence limits obtained from control subjects by calculating mean values + 2 standard deviations for VEP P100 IT and mean values − 2 standard deviations for PERG P50-N95 A, VEP N75-P100 A, MT, MV, and RNFL-T

	VA	MT			MV			RNFL					60′ PERG	60′ VEP		15′ PERG	15′ VEP	
	(LogMAR)	WR (μ)	IR (μ)	OR (μ)	WR (mm^3)	IR (mm^3)	OR (mm^3)	TT (μ)	ST (μ)	IT (μ)	NT (μ)	OT (μ)	A (μV)	IT (msec)	A (μV)	A (μV)	IT (msec)	A (μV)
#1	0.15	278	76	202	6.78	2.39	4.38	39	82	66	47	58.50	1.1	126	2.2	1.3	124	3.3
#2	0.04	260	59	200	6.91	2.15	4.75	36	71	76	42	56.23	1.5	136	3.5	1.4	132	6.3
#3	0.0	276	79	197	6.71	2.34	4.37	41	37	46	37	40.25	1.0	134	4.9	1.2	132	2.8
#4	0.4	257	64	193	6.82	2.46	4.36	57	58	81	56	63.00	1.2	131	4.6	1.5	128	4.7
#5	0.2	261	69	192	6.78	2.49	4.29	60	66	87	63	69.04	1.5	123	8.0	1.1	118	4.5
#6	0.0	253	61	192	6.93	2.31	4.61	36	70	78	61	61.25	1.6	138	3.7	1.6	138	6.5
#7	0.6	308	96	191	5.03	1.67	3.36	28	65	58	37	47.00	1.3	130	3.4	1.0	119	5.5
#8	0.0	367	92	250	7.81	2.98	4.82	64	73	98	61	74.00	1.6	130	6.9	1.6	132	5.7
#9	0.2	271	80	191	6.72	2.37	4.35	33	47	53	33	41.50	1.4	136	2.0	1.2	138	2.4
#10	0.04	269	77	191	6.54	2.26	4.28	42	65	85	31	55.75	1.6	137	2.4	1.5	129	2.8
#11	0.1	266	77	189	6.23	2.09	4.15	31	50	83	39	50.75	1.4	136	2.6	1.2	142	5.0
#12	0.04	260	71	189	6.70	2.44	4.26	60	66	64	52	60.50	1.6	118	8.2	1.2	119	7.3
#13	0.7	260	73	187	6.62	2.36	4.25	21	54	40	31	33.50	1.3	139	1.9	0.9	136	3.3
#14	0.0	244	61	183	6.82	2.53	4.29	73	71	62	51	64.25	1.6	122	6.8	1.8	117	12.4
#15	0.0	253	70	182	6.76	2.46	4.30	63	74	121	54	78.00	1.7	118	6.4	1.4	119	7.6
#16	0.15	232	51	181	6.26	2.09	4.17	36	56	77	53	55.50	1.2	133	2.4	1.0	136	2.2
#17	0.5	230	50	180	6.36	2.24	4.11	54	63	74	60	62.75	1.2	136	2.4	1.2	136	3.2
#18	0.7	289	103	179	6.74	2.48	4.26	70	86	93	54	75.75	1.7	128	9.1	1.6	118	7.8
#19	0.7	249	74	175	6.74	2.52	4.22	29	40	67	30	41.50	1.1	138	3.4	1.3	132	4.9
#20	0.0	246	72	175	6.80	2.36	4.44	35	39	67	38	44.75	1.3	134	2.4	1.3	131	3.2
#21	0.0	216	50	166	6.29	2.18	4.10	53	78	55	37	55.75	1.2	127	3.2	1.3	132	3.0
#22	0.0	223	59	164	6.56	2.46	4.10	57	67	67	47	59.50	1.3	129	2.3	1.3	118	3.9
95% CL		287.90	115.10	161.60	6.86	2.55	3.69	69.16	109.82	118.78	78.10	104.68	2.20	107.25	8.67	2.18	111.32	7.90

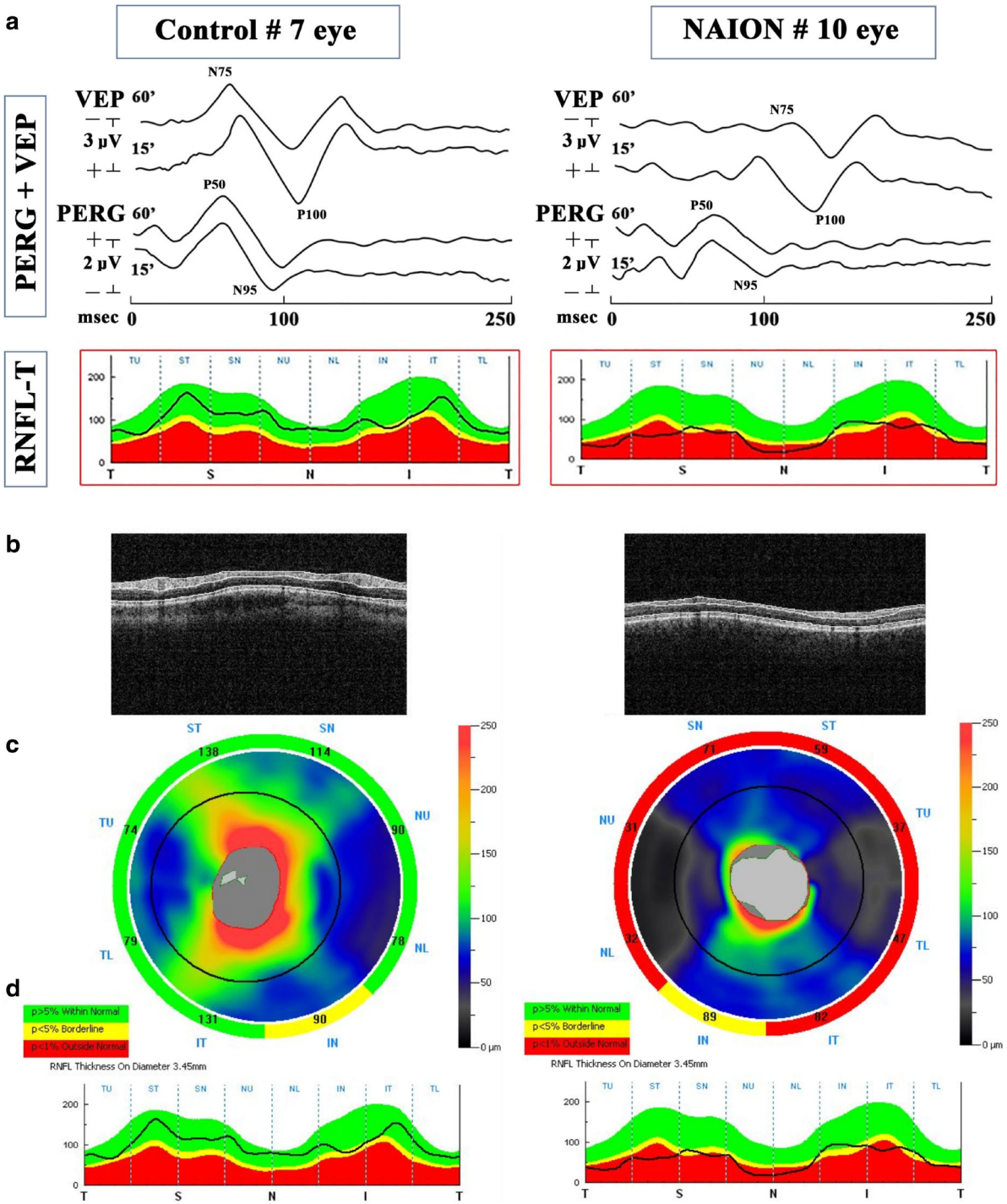

Fig. 1 Examples of simultaneous pattern electroretinogram (PERG) and visual evoked potential (VEP) (**a**) recordings and of retinal nerve fiber layer thickness (RNFL-T) (**b**–**d**) analysis observed in one representative control eye (#7) and one non-arteritic ischemic optic neuropathy (NAION) eye (#10). On panel **b**, the anatomical scan line of the boundaries between the vitreoretinal interface and the retinal pigment epithelium and the choriocapillaris is reported. On panel **c**, the analysis of the RNFL map for 8 quadrants is presented. On panel **d**, the thickness profile of RNFL for each sector is reported. We considered the average value of 8 different measurements per 4 quadrants (RNFL temporal, T (TU + TL/2); superior, S (ST + SN/2); nasal, N (NU+NL/2); inferior, I (IT+IN/2)); the overall data obtained in all quadrants (8 values averaged) was identified as RNFL overall (see Methods). A colorimetric scale of the RNFL thickness is presented on the right. 60′ and 15′ = check edges subtending 60 min (60′) and 15 min (15′) of the visual angle for PERG and VEP visual stimuli; N75 and P100 refer to the first negative and the first positive peak of VEP recordings (the peak to peak N75-P100 amplitude and the implicit time of P100 were considered); P50 and N95 refer to the first positive and the second negative peak of PERG recordings (the peak to peak P50-N95 amplitude was considered). In NAION eye, with respect to control eye, it is possible to observe reduced P50-N95 PERG amplitude, delayed P100 VEP implicit time, reduced N75-P100 VEP amplitude, and reduced RNFL-T

Table 2 Mean values of visual acuity (VA), macular thickness (MT), macular volume (MV), retinal nerve fiber layer (RNFL) thickness, 60′ and 15′ pattern electroretinogram (PERG) P50-N95 amplitude (A), visual evoked potentials (VEP) P100 implicit time (IT) and N75-P100 amplitude (A) detected in control eyes, in eyes with non-arteritic ischemic optic neuropathy (NAION), and in fellow eyes of NAION eyes (NAION-FE)

	Controls ($N = 20$)		NAION-FE ($N = 22$)		NAION ($N = 22$)		NAION Ab	% of Ab	ANOVA: NAION vs Controls		ANOVA: NAION vs NAION-FE	
	Mean	1SD	Mean	1SD	Mean	1SD			f (1,41) =	p =	f (1,43) =	p =
VA (LogMAR)	0.00	0.00	0.00	0.00	0.21	0.26	18	82	13.00	*	94.35	*
MT-WR (μ)	321.16	16.61	318.28	14.84	262.18	31.61	19	86	55.59	*	56.58	*
MT-IR (μ)	127.30	6.13	122.2	6.87	71.09	14.12	22	100	270.16	*	759.01	*
MT-OR (μ)	193.80	16.12	196.08	15.92	188.59	16.90	0	0	1.04	0.314	0.26	0.615
MV-WR (mm^3)	7.48	0.31	7.34	0.28	6.63	0.48	19	86	55.75	*	35.91	*
MV-IR (mm^3)	2.97	0.21	2.78	0.24	2.35	0.24	21	95	78.67	*	35.21	*
MV-OR (mm^3)	4.43	0.37	4.36	0.42	4.28	0.28	1	4	2.22	0.144	0.55	0.461
RNFL-TT (μ)	86.40	8.62	83.6	8.16	46.27	16.33	22	100	97.79	*	91.99	*
RNFL-ST (μ)	132.30	11.24	129.4	9.86	62.09	13.79	22	100	333.41	*	346.83	*
RNFL-IT (μ)	140.50	10.86	138.7	9.04	72.09	18.06	21	95	220.09	*	239.31	*
RNFL-NT (μ)	96.40	9.15	94.6	8.93	46.23	10.78	22	100	270.49	*	262.68	*
RNFL- OT (μ)	113.90	4.61	111.6	4.19	56.66	11.97	22	100	405.81	*	414.38	*
60′ PERG A (μV)	2.62	0.21	2.49	0.27	1.38	0.21	22	100	380.36	*	231.68	*
60′ VEP IT (msec)	100.51	3.37	101.03	4.03	130.86	6.39	22	100	365.43	*	243.00	*
60′ VEP A (μV)	12.43	1.88	12.54	2.13	4.21	2.29	21	95	164.88	*	156.07	*
15′ PERG A (μV)	2.74	0.28	2.69	0.32	1.31	0.22	22	100	359.97	*	277.83	*
15′ VEP IT (msec)	103.60	3.86	105.03	4.12	128.45	8.03	22	100	160.20	*	148.14	*
15′ VEP A (μV)	11.34	1.72	11.68	2.44	4.92	2.40	21	95	100.08	*	85.83	*

N number of eyes, *SD* standard deviation; *ANOVA* one-way analysis of variance; *p* values lower than 0.01 (*) were considered as statistically significant. *Ab* abnormal with respect to 95% normal confidence limits (mean values + 2 SD for VEP IT and mean values − 2 SD for PERG A, VEP A, RNFL-T, MT, and MV; VA was considered as Ab for values greater than 0.0 LogMAR); *60′ and 15′*, visual stimuli checks subtending 60 and 15 min of visual arc, respectively; *WR*, whole retina; *IR*, inner retina; *OR*, outer retina; *TT*, temporal thickness; *ST*, superior thickness; *IT*, inferior thickness; *NT*, nasal thickness; *OT*, overall thickness; *μ*, microns; *μV*, microvolt; *msec* milliseconds

On Table 1, individual data of VA, MT, MV, RNFL-T, PERG, and VEP from 22 NAION patients are presented. The number and the relative percentage of normal/abnormal values for each psychophysical, morphological, and functional parameter detected is reported in Table 2.

Table 3 Linear correlations (Pearson's test) between macular thickness (MT), macular volume (MV), retinal nerve fiber layer (RNFL) thickness and 60′ and 15′ pattern electroretinogram P50-N95 (PERG) amplitude (A), visual evoked potentials (VEP) P100 implicit time (IT) and N75-P100 amplitude (A) values detected in patients with non-arteritic ischemic optic neuropathy (NAION). *WR*, whole retina; *IR*, inner retina; *OR*, outer retina; *TT*, temporal thickness; *OT*, overall thickness; *60′ and 15′*, visual stimuli checks subtending 60 and 15 min of visual arc, respectively; *μ*, microns; *μV*, microvolt; *msec*, milliseconds. *p* values lower than 0.01 (*) were considered as statistically significant

	60′ PERG A (μV)		60′ VEP IT (msec)		60′ VEP A (μV)		15′ PERG A (μV)		15′ VEP IT (msec)		15′ VEP A (μV)	
	R	p =	R	p =	R	p =	R	p =	R	p =	R	p =
MT-WR (μ)	0.27	0.207	− 0.00	0.970	0.34	0.120	0.16	0.470	0.01	0.952	0.13	0.558
MT-IR (μ)	0.26	0.240	− 0.03	0.860	0.34	0.110	0.07	0.726	− 0.10	0.648	0.15	0.497
MT-OR (μ)	0.21	0.328	0.03	0.893	0.24	0.268	0.21	0.342	0.14	0.519	0.07	0.750
MV-WR (mm^3)	0.30	0.169	− 0.06	0.788	0.34	0.114	0.55	*	− 0.10	0.647	0.18	0.413
MV-IR (mm^3)	0.28	0.205	− 0.25	0.245	0.47	0.023	0.62	*	− 0.30	0.162	0.25	0.261
MV-OR (mm^3)	0.27	0.208	0.11	0.617	0.18	0.421	0.50	0.017	0.08	0.703	0.09	0.685
RNFL-TT (μ)	–	–	–	–	–	–	0.64	*	− 0.70	*	0.61	*
RNFL-OT (μ)	0.60	*	− 0.63	*	0.66	*	–	–	–	–	–	–

Table 4 Linear correlations (Pearson's test) between visual acuity (VA) and macular thickness (MT), macular volume (MV), retinal nerve fiber layer (RNFL) thickness, 60′ and 15′ pattern electroretinogram P50-N95 (PERG) amplitude (A), visual evoked potential (VEP) P100 implicit time (IT) and N75-P100 amplitude (A) values detected in patients with non-arteritic ischemic optic neuropathy (NAION). *p* values lower than 0.01 (*) were considered as statistically significant. *WR*, whole retina; *IR*, inner retina; *OR*, outer retina; *TT*, temporal thickness; *ST*, superior thickness; *IT*, inferior thickness; *NT*, nasal thickness; *OT*, overall thickness; *μ*, microns; *msec*, milliseconds; *μV*, microvolt; *60′ and 15′*, visual stimuli checks subtending 60 and 15 min of visual arc, respectively

	VA (LogMAR)	
	R	*p* =
MT-WR (μ)	0.098	0.662
MT-IR (μ)	0.343	0.117
MT-OR (μ)	− 0.169	0.451
MV-WR (mm^3)	− 0.411	0.057
MV-IR (mm^3)	− 0.684	*
MV-OR (mm^3)	− 0.395	0.068
RNFL-TT (μ)	− 0.618	*
RNFL-ST (μ)	− 0.309	0.160
RNFL-IT (μ)	− 0.189	0.397
RNFL-NT (μ)	− 0.231	0.299
RNFL-OT (μ)	− 0.423	0.049
60′ PERG A (μV)	− 0.306	0.164
60′VEP IT (msec)	0.672	*
60′ VEP A (μV)	− 0.355	0.104
15′ PERG A (μV)	− 0.584	*
15′VEP IT (msec)	0.684	*
15′ VEP A (μV)	− 0.148	0.510

On average, significant differences ($p < 0.01$) between NAION and NAION-FE or and control groups were detected for mean values of the following parameters: VA, MT-WR, MT-IR, MV-WR, MV-IR, RNFL-TT, RNFL-ST, RNFL-IT, RNFL-NT, RNFL-OT, 60′ PERG A, 60′ VEP IT and A, 15′ PERG A, 15′ VEP IT and A. Mean values of MT-OR and MV-OR were not significantly different ($p > 0.01$) between NAION, NAION-FE, and control groups. These results are reported in Table 2.

On Table 3, the linear correlation between morphological and functional data detected in NAION eyes is presented. Significant correlations ($p < 0.01$) between MV-WR, MV-IR, and 15′ PERG A were found. Moreover, RNFL-TO significantly ($p < 0.01$) correlated with 60′ PERG A, 60′ VEP IT, and 60′ VEP A; also, RNFL-TT correlated significantly ($p < 0.01$) with 15′ PERG A, 15′ VEP IT, and 15′ VEP A. No other significant correlations were found.

On Table 4, the linear correlations between VA values and both morphological and functional data observed in NAION eyes are presented. Significant ($p < 0.01$) correlations were found between VA and MV-IR, RNFL-TT, and both 60′ and 15′ VEP IT values. Moreover, 15′ PERG A values were significantly ($p < 0.01$) correlated with VA ones. No other significant correlations between morpho-functional and VA data were observed.

In addition, as represented in Fig. 2, no significant ($p > 0.01$) linear correlations between 60′ and 15′ PERG A findings and the corresponding values of 60′ and 15′ VEP IT were observed, whereas significant ($p < 0.01$) linear correlations between 60′ and 15′ PERG A findings and the corresponding values of 60′ and 15′ VEP A were found in NAION eyes.

Discussion

Our study aimed to assess the potential correlation between the macular and optic nerve fibers' morphological involvement and the RGCs and visual pathways' function, and to investigate whether the changes in VA might be related to the morpho-functional findings in the chronic phase of NAION.

When compared to controls and NAION-FE, NAION eyes showed a morphological impairment involving the whole retina and the inner retina of the macular region (significant reduction of MT-WR, MT-IR, MV-WR, and MV-IR), the peripapillary RNFL (significant reduction of RNFL-T overall and of all sectors), whereas no changes of the outer macular layers (not significantly reduced MT-OR and MV-OR) were found. In the same eyes, significant reduction of VA and abnormal electrophysiological responses (reduced 60′ and 15′ PERG A and VEP A and increased 60′ and 15′ VEP IT) was found.

These findings and their relationships are discussed separately as follows.

Macular and nerve fiber layer structural impairment and the correlation with VA changes

MT and MV, especially of the IR layers, although poorly used as a parameter to investigate on the effect of neurodegeneration in NAION eyes, may be considered a reliable surrogate for determining the extent of ischemic damage to the macular elements [15, 17, 18]. Our results (thinning of MT and MV of the WR and IR) are consistent with few other similar studies [13, 15, 17, 18] that described a significant decrease of MT-WR and MT-IR [15, 17] as well as thinning of MV-WR and MV-IR [15]. Indeed, the IR macular involvement has been better defined by using an accurate Sd-OCT segmentation that identified an involvement of GC-IPL [13, 16]. Our choice, instead, of

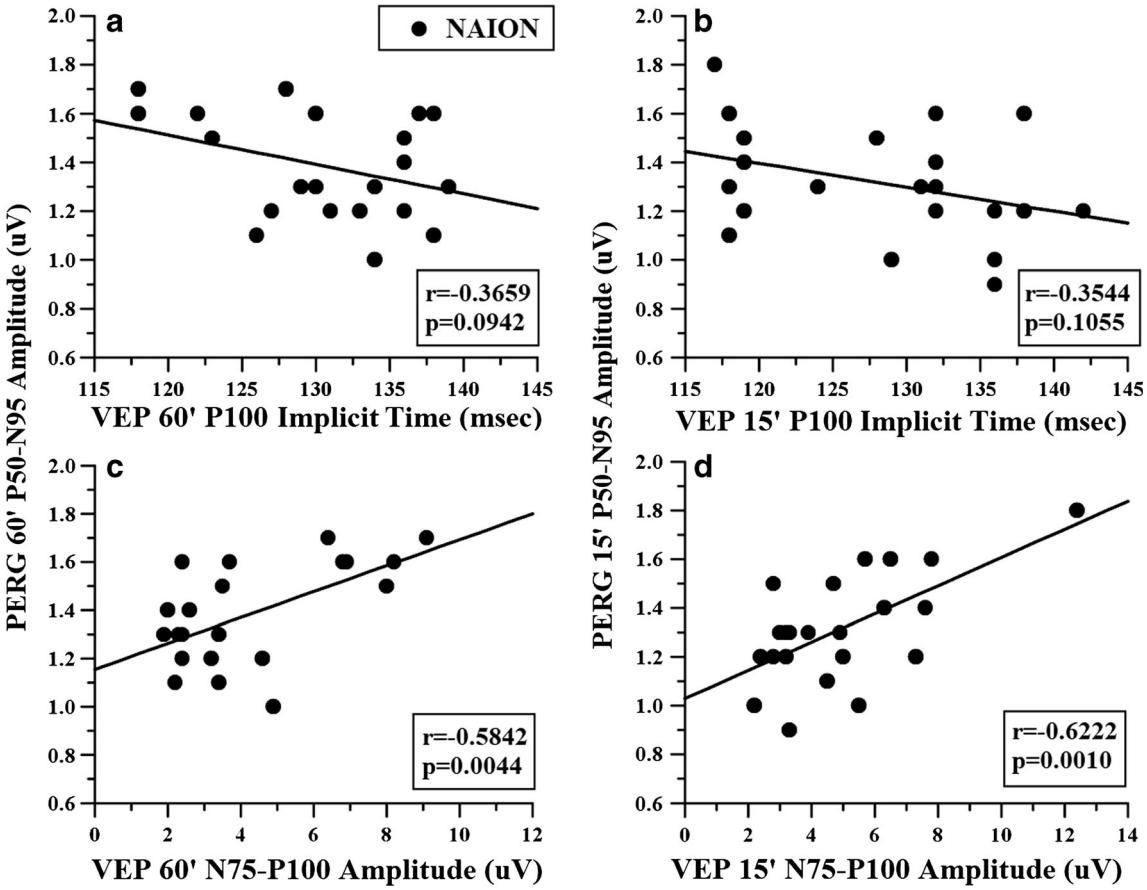

Fig. 2 Linear correlations (by Pearson's test) between 60′ pattern electroretinogram P50-N95 (PERG) amplitude and 60′ visual evoked potential (VEP) P100 implicit time (**a**) and N75-P100 amplitude (**c**) values, respectively, detected in patients with non-arteritic ischemic optic neuropathy (NAION). The linear correlations between 15′ P50-N95 PERG amplitude and 15′ VEP P100 implicit time and N75-P100 amplitude values are presented in **b** and **d** panels, respectively

measuring structural changes in NAION eyes by MT and MV resides on the possibility to further segment these parameters for measuring the OR and the IR layers. In particular, the segmentation of the IR (enclosing RNFL, RGCs layer, and IPL), which constitutes approximately 34% of the total averaged MT [38], allows to investigate on the axons, the RGCs bodies, and their dendrites located in specific layers that are thought to be damaged following the acute event of NAION [15]. In details, MT-IR and MV-IR include all neural retinal tissue and may capture the RGCs' loss, as a consequence of the ischemic effect inducing neurodegeneration of the macular IR [18].

Although there are several evidences on the involvement of IR in NAION [13–18], very few studies evaluated the OR morphology [15, 18]. Our finding of no significant difference MT-OR and MV-OR might indicate that OR structure may be preserved from the post-ischemic neurodegenerative process. However, Ackermann et al. [18] observed OR impairment in few macular regions and Papchenko et al. [15] described a significant reduction of MT-OR and MV-OR, suggesting loss of photoreceptors subsequent or concurrent with RGC death. Further studies about the macular OR structure in NAION should be useful for clarifying our and abovementioned contrasting findings.

In our study, no correlations between MT-WR, MT-IR, MT-OR, MV-WR, MV-OR, and VA were observed, as also found by Ackermann et al. [18]. Instead, Keller et al. [17] found a correlation between MT-IR and VA 1 month after the acute event, suggesting that the post-ischemic apoptosis of RGCs induces a retrograde degeneration of the deep retinal layers responsible for high-contrast VA. They also found a correlation between MT-OR and VA, suggesting that the optic nerve edema could damage the soma of photoreceptor cells by increasing compartmental pressure and leading to persistent ONL thickening that influences VA. By contrast, we observed that the individual values of VA were significantly correlated only with the corresponding values of reduced MV-IR. This is in agreement with the only work [15] that considered the same correlation. Our results suggest that, since the IR represents approximately one-third of the retinal thickness [38], MV-IR could be considered a parameter able to reflect RGC loss that might contribute to the neural damage responsible for VA loss. Indeed, we also observed reduced MV-IR in some

NAION eyes (see Table 1) with normal VA values (0.0 LogMAR). This could suggest that it is possible to find a preserved normal VA also in the presence of a morphological RGC impairment.

About the peripapillary RNFL, a significant decrease of overall and sectorial quadrants' thickness was observed in our NAION eyes compared to controls and NAION-FE. RNFL-T reduction represents the degeneration of RGCs' axons that results from the direct ischemic impact on the optic nerve head, as already described by several previous studies [2, 11, 14–16].

In summary, our results indicate that, although the primary site of damage is the optic nerve head, there is a loss of large part of the RGCs' axons (RNFL) with a concomitant morphological impairment of RGCs' bodies located in the macular region, and this could explain thinning of MT and MV [5]. Different authors [9, 10, 13] considered that the RGC damage happens earlier than the axonal loss. Our findings, as mentioned above, refer to the chronic phase of NAION without a longitudinal follow-up and therefore do not allow to establish whether the damage impairs earlier the RGCs or their axons [10].

In NAION eyes, VA loss showed a significant correlation with the reduction of RNFL-TT, whereas no correlations between overall and other sectorial RNFL-T and VA were found. These findings could be explained by the data that the morphological impairment of RNFL-TT might influence the central vision in NAION eyes, as VA deficit depends on the severity of the damage sustained by the papillomacular bundle [2, 11, 15, 26, 39], together with the abovementioned MV-IR impairment. By contrast, some NAION eyes can retain normal VA with concomitant reduced RNFL-TT, as presented on Table 1.

RGCs and visual pathways' dysfunction and their correlation with morphological and VA changes

Our NAION eyes showed reduced 60′ and 15′ PERG A when compared to controls and NAION-FE, consistent with previous other reports [4, 25, 26]. It is known that in humans, the integrity of the innermost retinal layers is required to obtain a normal PERG response, although a contribution of the retinal pre-ganglionic element function cannot be entirely excluded on the genesis of this bioelectrical activity [40–45]. On the basis of morpho-functional studies performed in neurodegenerative diseases involving the IR (i.e., multiple sclerosis [46], Alzheimer's disease [47], glaucoma [48]), we are confident that the P50-N95 amplitude could be the PERG component that better describes the IR function [23]. Therefore, the observed reduced 15′ PERG A indicates that IR is impaired in eyes affected by ischemic optic neuropathy. In addition, reduced 15′ PERG A was significantly correlated with the morphological impairment of MV-WR, MV-IR, and RNFL-TT. This finding, according to other previous correlations detected in other neurodegenerative diseases (see for a review Parisi [49]), is a further evidence that, also in humans, PERG A is dependent from the morphological integrity of the innermost retinal layers. This is supported by the lack of correlation between 15′ PERG A, MT-OR, and MV-OR. However, differently from the pathogenesis of other neurodegenerative diseases [49], the IR dysfunction (reduced 15′ PERG A) is likely to be due to the long-term effects of insufficient vascular blood supply at the optic nerve head level that may produce a direct damage on the RGCs' bodies and their fibers. However, since reduced 15′ PERG A was correlated significantly with both reduced RNFL-TT and MV-IR, we cannot uniquely establish whether, in the chronic phase, this dysfunction is due to post-ischemic retrograde degeneration or rather to the direct hypoxic impact on the RGCs. All this applies only to the 15′ PERG stimulus that preferentially activates the RGCs located in the macula. It is likely that, when using larger checks (60′ stimulus), the obtained transient PERG signal captures also the response from those retinal elements sensitive to uniform luminance changes (pre-ganglionic cells located in more distal retinal layers) [21, 37]. This is also supported by the lack of correlation between 60′ PERG A and MT/MV-IR.

The data that the 15′ PERG A impairment was significantly correlated with both RNFL-TT and VA confirms that reduced VA in our NAION patients depends on the impaired morpho-functional condition of the IR [49].

In previous studies of NAION [50–53], reduced VEP amplitudes were observed also in presence of normal ITs and this was ascribed to the fact that a sectorial optic nerve ischemic injury cannot affect the timing of the neural conduction, being, however, the bioelectrical responses reduced at the level of visual cortex. By contrast, our NAION eyes showed significant delayed VEP IT and reduced amplitudes, in agreement with other previous findings [4, 5, 22, 23], leading us to believe that the optic nerve ischemic damage affects both the timing of the neural conduction along the visual pathways and the entity of the visual cortical responses. The first was independent from the bioelectric activity of the RGCs (lack of correlation between PERG A and VEP IT), whereas the latter was influenced by the RGC impairment (correlation between PERG A and VEP A).

VEP responses were obtained by using different spatial frequencies with larger or smaller checks (60′ and 15′, respectively) to obtain information on the function of large and small axons forming the visual pathways, respectively [19–21]. This is supported by the significant correlation between RNFL-OT with 60′ VEP IT and A, and the relationship between RNFL-TT with 15′ VEP IT and A. Since our patients were evaluated in the chronic phase, the abovementioned correlated morpho-functional findings could be ascribed to long-term neurodegenerative process, due to ischemia inducing loss/dysfunction

of both small and large axons forming the optic nerve. Accordingly, in our NAION patients, we found that VA changes were dependent from the impaired neural conduction along both large and small axons composing the visual pathways (60′ and 15′ delayed VEP IT).

In conclusion, the novelty of our findings consisted in assessing and correlating the morphological, functional, and the VA changes in patients with chronic NAION. We found that, in this phase on the disease, there is a morpho-functional impairment of the IR, with OR structural sparing. VA changes were related to the impaired morphology and function of IR (reduced MV-IR and 15′ PERG A), to the RNFL-TT defects and to a dysfunction of the neural conduction along the visual pathway (delayed or reduced VEP responses).

Acknowledgments Research for this study was supported in part by the Italian Ministry of Health and in part by Fondazione Roma. Authors acknowledge Dr. Valter Valli Fiore and Maria Luisa Alessi for technical help in electrophysiological recordings and graphics, Dr. Federica Petrocchi for executing psychophysical test, and Dr. Ester Elmo for critical revision of the bibliography.

Authors' contributions Conception and design: VP; analysis and interpretation: VP, LB, LZ; review and discussion: VP, LB, LZ; data collection: VP, LB; overall responsibility: VP.

Data availability Data and material are available upon request.

Compliance with ethical standards

Conflict of interest The authors declare that they have no conflict of interest.

Ethics approval All procedures performed in this study were in accordance with the ethical standards of the institutional and/or national research committee and with the 1964 Helsinki Declaration and its later amendments or comparable ethical standards. This research was approved by the local ethics committee on February 14, 2017 (Comitato Etico Centrale IRCCS Lazio, Sezione IFO/Fondazione Bietti, Rome, Italy).

Consent to participate Informed consent was obtained from all individual participants included in the study.

Consent for publication Each patient consented for data publication.

Proprietary interest None of the author has proprietary interest in the content of the manuscript.

References

1. Mathews MK (2005) Nonarteritic anterior ischemic optic neuropathy. Curr Opin Ophthalmol 16:341–345
2. Contreras I, Noval S, Rebolleda G, Muñoz-Negrete FJ (2007) Follow-up of nonarteritic anterior ischemic optic neuropathy with optical coherence tomography. Ophthalmology 114:2338–2344
3. Huang-Link YM, Al-Hawasi A, Lindehammar H (2015) Acute optic neuritis: retinal ganglion cell loss precedes retinal nerve fiber thinning. Neurol Sci 36:617–620
4. Parisi V, Gallinaro G, Ziccardi L, Coppola G (2008) Electrophysiological assessment of visual function in patients with non-arteritic ischaemic optic neuropathy. Eur J Neurol 15:839–845
5. Parisi V, Barbano L, Di Renzo A, Coppola G, Ziccardi L (2019) Neuroenhancement and neuroprotection by oral solution citicoline in non-arteritic ischemic optic neuropathy as a model of neurodegeneration: a randomized pilot study. PLoS One 14:e0220435
6. Rebolleda G, Diez-Alvarez L, Casado A et al (2015) OCT: new perspectives in neuro-ophthalmology. Saudi J Ophthalmol 29:9–25
7. Ishikawa H, Stein DM, Wollstein G, Beaton S, Fujimoto JG, Schuman JS (2005) Macular segmentation with optical coherence tomography. Invest Ophthalmol Vis Sci 46:2012–2017
8. Bellusci C, Savini G, Carbonelli M, Carelli V, Sadun AA, Barboni P (2008) Retinal nerve fiber layer thickness in nonarteritic anterior ischemic optic neuropathy: OCT characterization of the acute and resolving phases. Graefes Arch Clin Exp Ophthalmol 246:641–647
9. Akbari M, Abdi P, Fard MA et al (2016) Retinal ganglion cell loss precedes retinal nerve fiber thinning in nonarteritic anterior ischemic optic neuropathy. J Neuroophthalmol 36:141–146
10. Kupersmith MJ, Garvin MK, Wang JK, Durbin M, Kardon R (2016) Retinal ganglion cell layer thinning within one month of presentation for non-arteritic anterior ischemic optic neuropathy. Invest Ophthalmol Vis Sci 57:3588–3593
11. Dotan G, Goldstein M, Kesler A, Skarf B (2013) Long-term retinal nerve fiber layer changes following nonarteritic anterior ischemic optic neuropathy. Clin Ophthalmol 7:735–740
12. Han M, Zhao C, Han QH, Xie S, Li Y (2016) Change of retinal nerve layer thickness in non-arteritic anterior ischemic optic neuropathy revealed by Fourier domain optical coherence tomography. Curr Eye Res 41:1076–1081
13. Larrea BA, Iztueta MG, Indart LM, Alday NM (2014) Early axonal damage detection by ganglion cell complex analysis with optical coherence tomography in nonarteritic anterior ischaemic optic neuropathy. Graefes Arch Clin Exp Ophthalmol 252:1839–1846
14. Aggarwal D, Tan O, Huang D, Sadun AA (2012) Patterns of ganglion cell complex and nerve fiber layer loss in nonarteritic ischemic optic neuropathy by Fourier-domain optical coherence tomography. Invest Ophthalmol Vis Sci 53:4539–4545
15. Papchenko T, Grainger BT, Savino PJ, Gamble GD, Danesh-Meyer HV (2012) Macular thickness predictive of visual field sensitivity in ischaemic optic neuropathy. Acta Ophthalmol 90:e463–e469
16. Gonul S, Koktekir BE, Bakbak B, Gedik S (2013) Comparison of the ganglion cell complex and retinal nerve fibre layer measurements using Fourier domain optical coherence tomography to detect ganglion cell loss in non-arteritic anterior ischaemic optic neuropathy. Br J Ophthalmol 97:1045–1050
17. Keller J, Oakley JD, Russakoff DB, Andorrà-Inglés M, Villoslada P, Sánchez-Dalmau BF (2016) Changes in macular layers in the early course of non-arteritic ischaemic optic neuropathy. Graefes Arch Clin Exp Ophthalmol 254:561–567
18. Ackermann P, Brachert M, Albrecht P et al (2017) Alterations of the outer retina in non-arteritic anterior ischaemic optic neuropathy detected using spectral-domain optical coherence tomography. Clin Exp Ophthalmol 45:496–508
19. Parisi V, Ziccardi L, Sadun F et al (2019) Functional changes of retinal ganglion cells and visual pathways in patients with Leber's hereditary optic neuropathy during one year of follow-up in chronic phase. Ophthalmology 126:1033–1044
20. Parisi V, Scarale ME, Balducci N, Fresina M, Campos EC (2010) Electrophysiological detection of delayed postretinal neural conduction in human amblyopia. Invest Ophthalmol Vis Sci 51:5041–5048
21. Ziccardi L, Sadun F, De Negri AM et al (2013) Retinal function and neural conduction along the visual pathways in affected and unaffected carriers with Leber's hereditary optic neuropathy. Invest Ophthalmol Vis Sci 54:6893–6901

22. Janáky M, Fülöp Z, Pálffy A, Benedek K, Benedek G (2006) Electrophysiological findings in patients with nonarteritic anterior ischemic optic neuropathy. Clin Neurophysiol 117:1158–1166
23. Atilla H, Tekeli O, Ornek K, Batioglu F, Elhan AH, Eryilmaz T (2006) Pattern electroretinography and visual evoked potentials in optic nerve diseases. J Clin Neurosci 13:55–59
24. Almárcegui C, Dolz I, Alejos MV, Fernández FJ, Valdizán JR, Honrubia FM (2001) Pattern electroretinogram in anterior ischemic optic neuropathy. Rev Neurol 32:18–21
25. Froehlich J, Kaufman DI (1994) Use of pattern electroretinography to differentiate acute optic neuritis from acute anterior ischemic optic neuropathy. Electroencephalogr Clin Neurophysiol 92:480–486
26. Deleón-Ortega J, Carroll KE, Arthur SN, Girkin CA (2007) Correlations between retinal nerve fiber layer and visual field in eyes with nonarteritic anterior ischemic optic neuropathy. Am J Ophthalmol 143:288–294
27. Dotan G, Kesler A, Naftaliev E, Skarf B (2015) Comparison of peripapillary retinal nerve fiber layer loss and visual outcome in fellow eyes following sequential bilateral non-arteritic anterior ischemic optic neuropathy. Curr Eye Res 40:632–637
28. Wilhelm B, Lüdtke H, Wilhelm H (2006) Efficacy and tolerability of 0.2% brimonidine tartrate for treatment of acute non-arteritic anterior ischemic optic neuropathy (NAION): a 3-month, double-masked, randomised, placebo-controlled trial. Graefes Arch Clin Exp Ophthalmol 244:551–558
29. Parisi V, Centofanti M, Gandolfi S et al (2014) Effects of coenzyme Q10 in conjunction with vitamin E on retinal-evoked and cortical-evoked responses in patients with open-angle glaucoma. J Glaucoma 23:391–404
30. Spadea L, Dragani T, Magni R, Rinaldi G, Balestrazzi E (1996) Effect of myopic excimer laser photorefractive keratectomy on the electrophysiologic function of the retina and optic nerve. J Cataract Refract Surg 22:906–909
31. Celesia GG, Kaufman D (1985) Pattern ERGs and visual evoked potentials in maculopathies and optic nerve diseases. Invest Ophthalmol Vis Sci 26:726–735
32. Cruz-Herranz A, Balk LJ, Oberwahrenbrock T et al (2016) IMSVISUAL consortium. The APOSTEL recommendations for reporting quantitative optical coherence tomography studies. Neurology 86:2303–2309
33. Ziccardi L, Parisi V, Giannini D et al (2015) Multifocal VEP provide electrophysiological evidence of predominant dysfunction of the optic nerve fibers derived from the central retina in Leber's hereditary optic neuropathy. Graefes Arch Clin Exp Ophthalmol 253:1591–1600
34. Odom JV, Bach M, Brigell M, Holder GE, McCulloch DLL, Mizota A et al (2016) ISCEV standard for clinical visual evoked potentials – (2016 update). Doc Ophthalmol 133:1–9
35. Hawlina M, Konec B (1992) New non-corneal HK-loop electrode for clinical electroretinography. Doc Ophthalmol 81:253–259
36. Porciatti V, Falsini B (1993) Inner retina contribution to the flicker electroretinogram: a comparison with the pattern electroretinogram. Clin Vision Sci 8:435–447
37. Parisi V, Miglior S, Manni G, Centofanti M, Bucci MG (2006) Clinical ability of pattern electroretinograms and visual evoked potentials in detecting visual dysfunction in ocular hypertension and glaucoma. Ophthalmology 113:216–228
38. Burkholder BM, Osborne B, Loguidice MJ et al (2009) Macular volume determined by optical coherence tomography as a measure of neuronal loss in multiple sclerosis. Arch Neurol 66:1366–1372
39. Rebolleda G, Sánchez-Sánchez C, González-López JJ, Contreras I, Muñoz-Negrete FJ (2015) Papillomacular bundle and inner retinal thicknesses correlate with visual acuity in nonarteritic anterior ischemic optic neuropathy. Invest Ophthalmol Vis Sci 56:682–692
40. Holder GE (1997) The pattern electroretinogram in anterior visual pathways dysfunction and its relationship to the pattern visual evoked potential: a personal clinical review of 743 eyes. Eye 11:924–934
41. Holder GE (1987) The significance of abnormal pattern electroretinography in anterior visual pathway dysfunction. Br J Ophthalmol 71:166–171
42. Viswanathan S, Frishman LJ, Robson JG (2000) The uniform field and pattern ERG in macaques with experimental glaucoma: removal of spiking activity. Invest Ophthalmol Vis Sci 41:2797–2810
43. Holder GE, Votruba M, Carter AC et al (1999) Electrophysiological findings in dominant optic atrophy (DOA) linked to the OPA1 locus on chromosome 3q 28-qter. Doc Ophthalmol 95:217–228
44. Harrison JM, O'Connor PS, Young RS, Kincaid M, Bentley R (1993) The pattern ERG in man following surgical resection of the optic nerve. Invest Ophthalmol Vis Sci 28:492–499
45. Porciatti V (2015) Electrophysiological assessment of retinal ganglion cell function. Exp Eye Res 141:164–170
46. Parisi V, Manni G, Spadaro M et al (1999) Correlation between morphological and functional retinal impairment in multiple sclerosis patients previously affected by optic neuritis. Invest Ophthalmol Vis Sci 40:2520–2528
47. Parisi V, Restuccia R, Fattapposta F et al (2001) Morphological and functional retinal impairment in Alzheimer's disease patients. Clin Neurophysiol 112:1860–1867
48. Parisi V, Manni G, Centofanti M et al (2001) Correlation between optical coherence tomography, pattern electroretinogram, and visual evoked potentials in open-angle glaucoma patients. Ophthalmology 108:905–912
49. Parisi V (2003) Correlation between morphological and functional retinal impairment in patients affected by ocular hypertension, glaucoma, demyelinating optic neuritis and Alzheimer's disease. Semin Ophthalmol 18:50–57
50. Holder GE (2004) Electrophysiological assessment of optic nerve disease. Eye 18:1133–1143
51. Wilson WB (1978) Visual evoked response differentiation of ischaemic optic neuritis from the optic neuritis of multiple sclerosis. Am J Ophthalmol 86:530–535
52. Holder GE (1981) The visual evoked potential in ischaemic optic neuropathy. Doc Ophthalmol Proc Ser 27:123–129
53. Wildberger H (1984) Pattern-evoked potentials and visual field defects in ischaemic optic neuropathy. Doc Ophthalmol Proc Ser 40:193–201